ACS OMEGA

http://pubs.acs.org/journal/acsodf

Article

Experiment on the Scaling Mechanism of Strong Alkaline−Surfactant−Polymer in a Sandstone Reservoir

Runnan Zhou, Huiying Zhong,* Peng Ye, Jianguang Wei, Dong Zhang, Lianbin Zhong, and Tianyu Jiao

Cite This: *ACS Omega* 2022, 7, 1794−1802

Read Online

ACCESS | Metrics & More | Article Recommendations

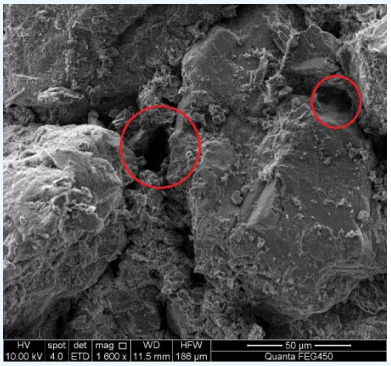

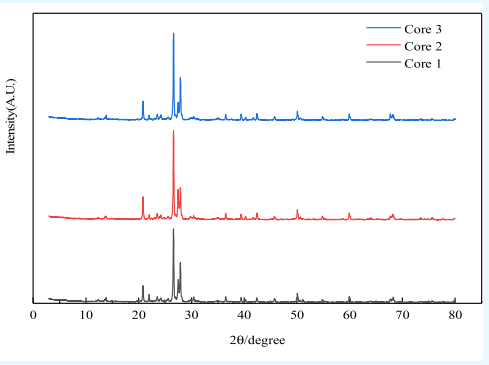

ABSTRACT: Most of the mature oilfields are facing the problem of great difficulty in exploitation currently. Alkaline−surfactant−polymer (ASP) flooding has been widely used in Daqing Oilfield as a tertiary oil recovery technology that can effectively enhance oil recovery (EOR). However, various degrees of scaling appeared in field application tests, which hindered the large-scale application of this technology. The damage and scaling mechanisms of strong alkali−surfactant−polymer (SASP) flooding to heterogeneous reservoirs with high clay mineral content are still unclear. In this study, several sets of experiments have been carried out to determine the core mineral composition and the pore structure. Additionally, the damage mechanism and mineral corrosion with different permeabilities can be explored from a microscopic point of view. The results indicate that the corrosion of SASP reduces the contents of quartz and kaolinite, while the illite/montmorillonite mixed layer increases. In addition, there is chlorite and secondary quartz generation, which do not exist in the original mineral composition. Clay particles and sediment are easy to form bridges or stay on the surface and block the pore throats, which results in core seepage capacity reduction. All our preliminary results have contributed to the present understanding of scaling during ASP flooding. Moreover, it is of great significance to guide ASP flooding field application and prevent scaling.

1. INTRODUCTION

With the exploitation of crude oil, most oilfields in China have entered the later stage of development, with high moisture content and low oil recovery.[1] After chemical flooding, serious heterogeneity and prominent interlayer contradictions present great challenges for further enhanced oil recovery (EOR) in most Chinese oilfield reservoirs. A large amount of remaining oil is retained in the reservoir and becomes more difficult to extract.[2−4] As the world's energy consumption continues to increase, traditional methods can no longer meet the needs of production.[5−7] Conventional methods including primary and secondary oil recovery can recover only 30% of the global original oil in place (OOIP) on average.[8] To further improve oil recovery, traditional methods must be replaced by tertiary oil recovery.[9−11] It is an effective way to produce additional original oil in place (OOIP) by physical and chemical techniques upon water flooding.[12] Qualitative methods including industrial and laboratory experiments have proved that tertiary oil recovery technology can effectively increase oil recovery by 5−20% upon water flooding.[13−15] Many researchers have utilized it as one of the most effective ways to enhance oil recovery in most old oilfields.

Most of the developed oilfields in China are at the end of the second stage. Heterogeneity is an important feature of many mature oilfields in Daqing Oilfield. It is analyzed that more than 60% of the oil is still trapped in the reservoir, which also poses a huge challenge to further enhance oil recovery.[16,17] There is a large amount of oil left because the remaining oil is

Received: September 7, 2021
Accepted: December 17, 2021
Published: January 4, 2022

https://doi.org/10.1021/acsomega.1c04925
ACS Omega 2022, 7, 1794−1802

either from water-swept areas or zones bypassed by water displacement.[18] Compared with screening criteria,[19] ASP flooding was most suitable for Daqing Oilfield according to the basic physical parameters of Daqing Oilfield after water flooding. It reduces the oil−water interfacial tension, increases the viscosity of the displacement phase, and reduces the water−oil mobility ratio through the synergistic effect of alkali, surfactants, and polymers, thereby greatly improving oil recovery.[20] Alkali plays an important role in maintaining the pH value of the solution, ensuring the surfactant and the polymer work at optimum conditions.[21,22] In addition, the chemical agents can work synergistically in improving oil recovery, and as a result, the amount of each chemical is reduced.[23−25]

Although ASP flooding can effectively improve recovery.[26] Scaling is a major problem both in the formation near the well or in the injection−production system, causing blockage of surface pipelines. The scaling problem impacts negatively upon the normal production and application.[27] This phenomenon is more obvious in Daqing Oilfield. The pump jam occurred after ASP flooding, both the oil suction pipe and the inner wall of the oil pipe were covered with a white dense substance. One of the main obstacles to the popularization and application of ASP flooding is scaling in oil wells.[28,29]

The scaling phenomenon has been conducted by many experts from scientific research institutes over the past decade. Previous research has established that the original equilibrium state of the reservoir would be destroyed, and the chemical reaction and the physical change occur between fluid and mineral components, resulting in the phenomenon of scaling.[30,31] Extensive research has shown that carbonate and silicate are the main components of the scale after ASP flooding.[32−34] The scale components and the core damage mechanism have been investigated quite intensively in recent years.

There are small amounts of clay minerals kaolinite and illiterate in the rocks. Dorothy has studied that NaOH has a more strong effect on kaolinite than that on montmorillonite and illite.[35] Previous studies ignore the influence of core composition before SASP flooding. Furthermore, little attention has been focused on the influence of core permeability and flow capacity after scaling. In addition, the experimental cores used for mineral composition analysis were mostly taken from different wells. Thus, these previous results may show some uncertainties.

In this study, several sets of experiments have been carried out to determine the core mineral composition and the pore structure. This is the first project to provide new insights into the original reservoir composition. Qualitative and quantitative research designs were adopted to show the influence on core seepage capacity after ASP flooding. The results also provide an important opportunity to advance the damage mechanism and mineral corrosion with different permeabilities from a microscopic point of view. Therefore, this comprehensive study makes major theoretical guidance for the effective development of SASP flooding.

2. RESULTS AND DISCUSSION

2.1. Seepage Experiment Results. The first set of analyses examined the impact of seepage capacity after SASP flooding. The core basic parameters and the results of permeability changes are shown in Table 1. Figure 1 shows the experimental data on the injection pressure change with the increase of injection volume.

Table 1. Physical Core Test Parameters of Permeability Changes

core number	permeability before flooding (mD)	porosity (%)	permeability after flooding (mD)	permeability loss (%)
1	309	23.1	237	23.3
2	762	25.4	669	12.2
3	1635	26.7	1517	8.9

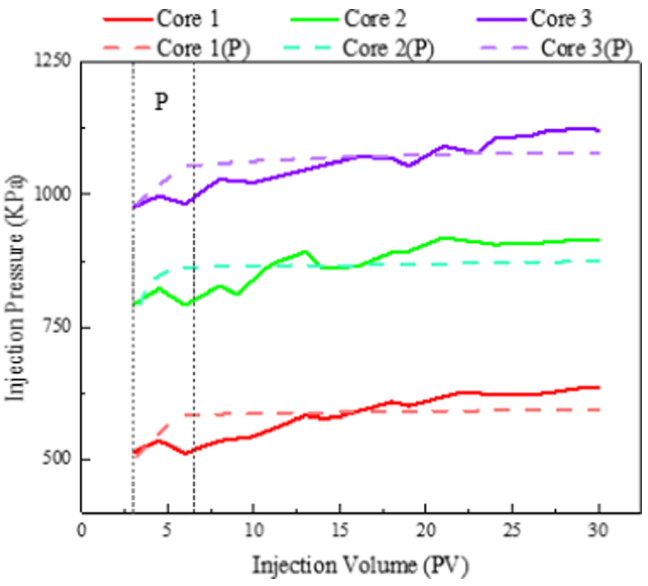

Figure 1. Curve of injection pressure with injection volume (Core 1(P), Core 2(P), and Core 3(P): only the polymer was injected).

The results of correlational analysis are presented in Figure 1. It is apparent from this curve that the injection pressure fluctuates and the seepage capacity is unstable at the beginning of SASP flooding. The most interesting aspect is that the injection pressure increased significantly after 30 PV was injected. Then, the injection pressure remained stable in the subsequent SASP flooding. Previous studies suggested that polymer retention also led to permeability reduction.[36,37] From Figure 1, we can conclude that the difference between two curves is the permeability change effect by scaling.

Further analysis showed that the seepage capacity is reduced after SASP flooding. The core with lower permeability will suffer more serious reservoir damage, which leads to the permeability and seepage capacity decrease.

2.2. Results of Pore Size Analysis. In the flooding experiment, SASP flooding was found to cause a decrease in permeability and seepage capacity. Previous studies evaluated that the reservoirs were scaled and core pores were damaged by the strong alkali in ASP flooding, which may be the main reason for the decrease of core permeability.

Therefore, to further explore the pore size changes after SASP flooding, high-pressure mercury intrusion tests were performed on the cores before and after the experiment. The experiment result of pore size is shown in Figure 2. The characteristic parameters of the pore structure are presented in Table 2.

https://doi.org/10.1021/acsomega.1c04925
ACS Omega 2022, 7, 1794−1802

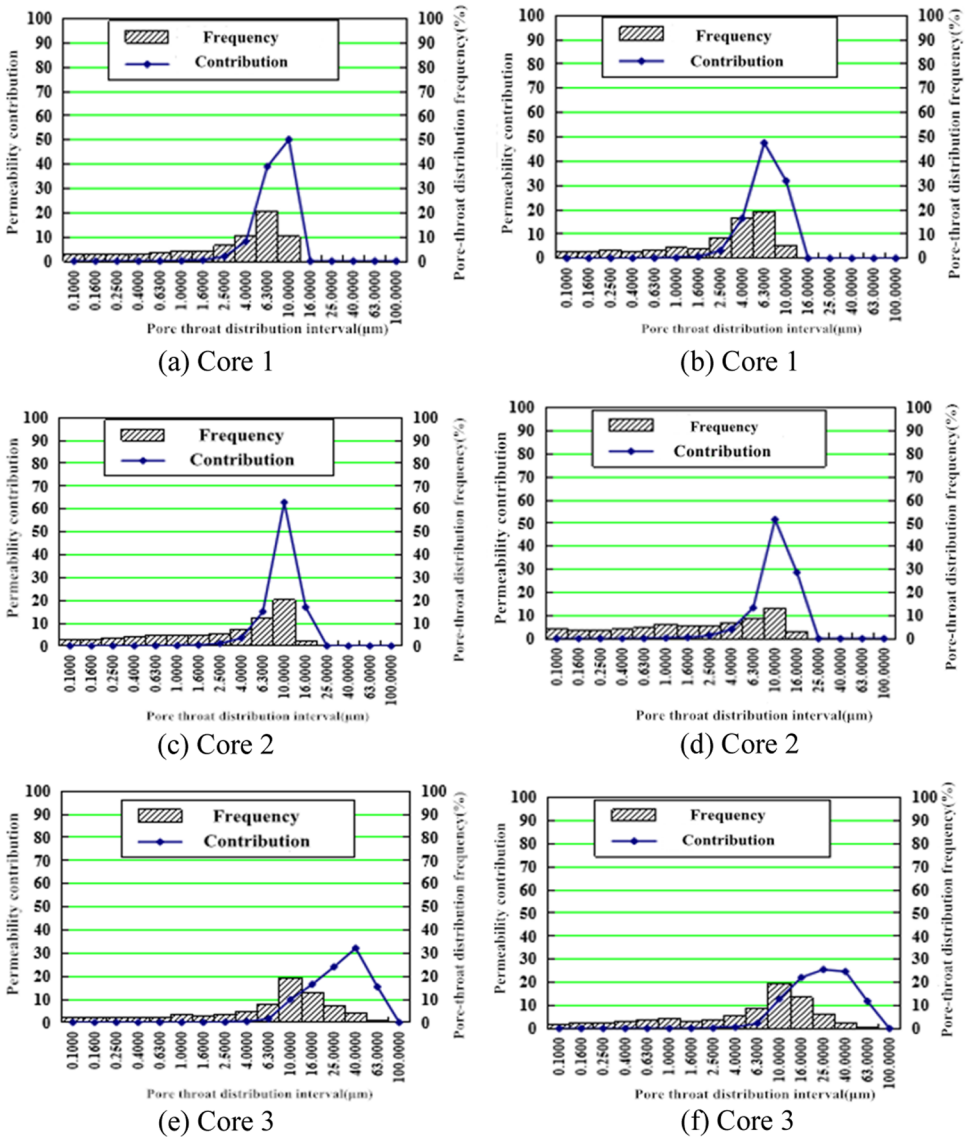

Figure 2. High-pressure mercury intrusion experiment results ((a, c, e) before and (b, d, f) after SASP flooding).

Table 2. Parameters of the Core Pore Structure

		test parameters			
core number	experimental program	average pore radius (μm)	maximum pore radius (μm)	sorting factor	structure factor
1	before flooding	12.87	33.8	2.63	0.626
	after flooding	12.10	28.3	2.23	1.212
2	before flooding	18.40	41.9	3.39	0.897
	after flooding	20.82	32.7	3.31	1.06
3	before flooding	25.00	59.4	6.26	1.551
	after flooding	29.63	51.0	5.71	1.418

From Figure 2, we can see that as the core permeability is 0.309 μm^2, the distribution frequency is highest at a pore partition of 6.3 μm, and the permeability contribution value is largest at a pore partition of 10 μm, which is close to 50%. After SASP flooding, the frequency of pore throat distribution at 4 μm is obviously increased, while at 10 μm, it is significantly reduced. Interestingly, both the highest distribution frequency and permeability contribution are at a pore partition of 6.3 μm.

As the core permeability is 0.762 μm^2, both the highest distribution frequency and permeability contribution are at a pore partition of 10 μm both before and after the SASP flooding experiment. The distribution frequency of pore throats less than 10 μm tends to be evenly distributed.

The distribution frequency is highest at a pore partition of 10 μm with a core permeability of 1.635 μm^2, while the permeability contribution value is largest at a pore partition of 40 μm. Most pore throats are distributed in the range of 10−25 μm. The distribution frequency of pore throats is basically unchanged compared with that before SASP flooding. The permeability contribution value is largest at a pore partition of 25 μm. The contribution of permeability increases the most at 16 μm, while decreases the most at 40 μm.

From the data listed in Table 2, there is a clear decreasing trend in the maximum pore radius and sorting factor. The cores with different permeabilities showed different features in the average pore radius and structure factors.

https://doi.org/10.1021/acsomega.1c04925
ACS Omega 2022, 7, 1794−1802

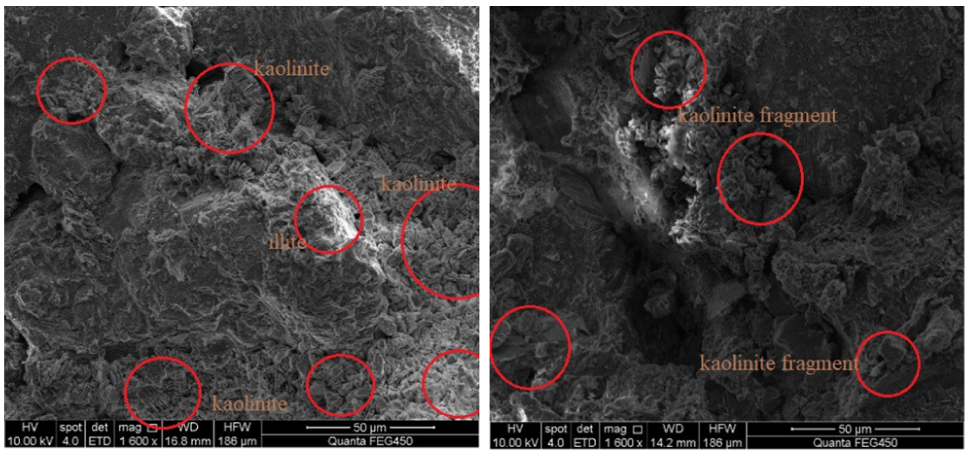

Figure 3. SEM results of kaolinite ((a) before and (b) after SASP flooding).

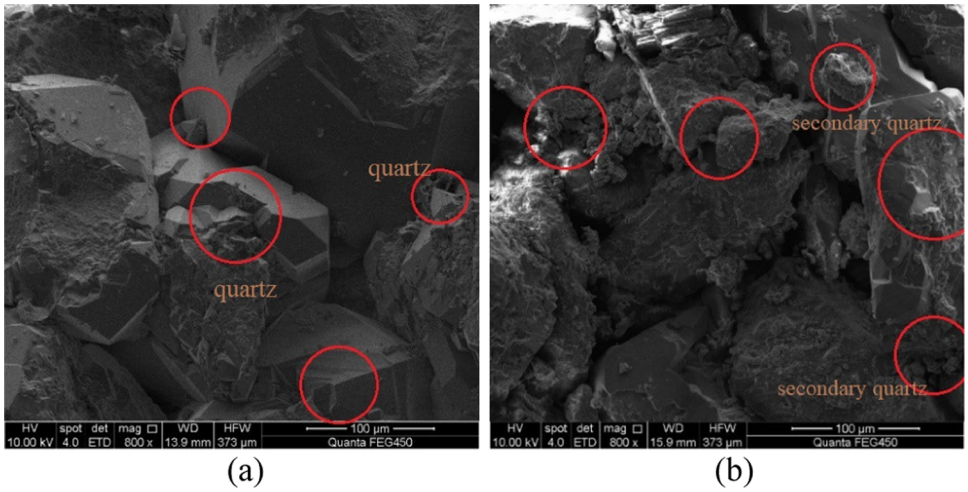

Figure 4. SEM results of quartz ((a) before and (b) after SASP flooding).

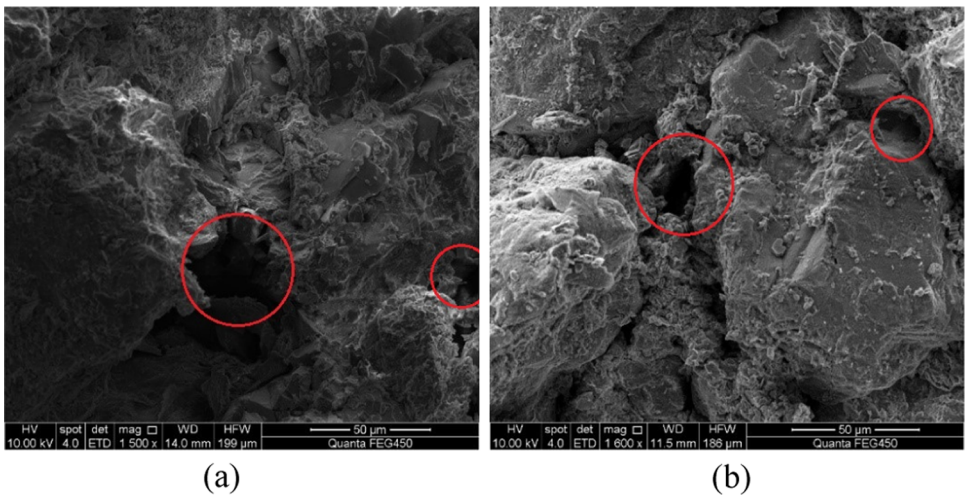

Figure 5. SEM results of the core sample ((a) before and (b) after SASP flooding).

The results of this study indicate that the peak of pore distribution shifts to the right, the distribution of large pores increases, and the heterogeneity of the pore structure becomes weaker. The size of large pores increases, the distribution of small pores tends to be uniform, the proportion decreases, and the connectivity of pore throats becomes worse after SASP flooding. Furthermore, the decrease of the sorting factor indicates that the core has a reduced effect on the displaced phase in the same displacement, which reduces the possibility of "finger protruding" and channeling. A possible explanation

https://doi.org/10.1021/acsomega.1c04925
ACS Omega 2022, 7, 1794−1802

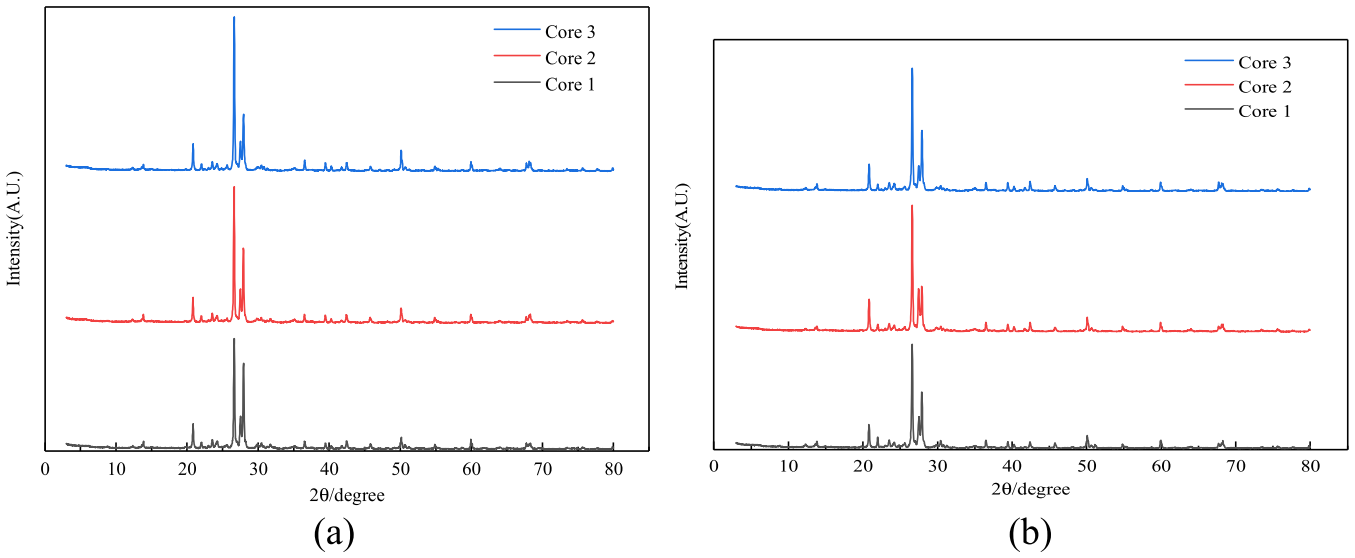

Figure 6. XRD experiment results ((a) before and (b) after SASP flooding).

Table 3. Mineral Composition Results

		test parameters (%)						
		clay mineral					matrix mineral	
core number	experimental program	illite/montmorillonite	illite	kaolinite	chlorite	total	quartz	feldspar
1	before flooding	0.3	0.9	7.9	0	9.1	41.3	49.2
	after flooding	7.6	0.9	4.7	2.5	15.7	36.3	47.8
2	before flooding	0.1	0.5	5.9	0	6.5	48.8	44.6
	after flooding	5.7	0.6	3.8	1.3	11.4	43.6	44.7
3	before flooding	0.1	0.2	5.3	0	5.6	54.6	39.5
	after flooding	5.8	0.3	3.3	0.9	10.3	50.9	38.6

for this might be the corrosion of alkali. Detrital particles or secondary mineral particles produced by corrosion migrate to form bridges or stay on the surface of pores, leading to the blockage of pore throats. The present study raises the possibility that the original seepage channel is changed by corrosion, thereby increasing the degree of curvature in the pores and making the seepage ability of the fluid in the pores worse. This result is in line with the conclusions of seepage experiments.

2.3. Results of SEM Analysis. To compare the difference in the microstructure during the SASP flooding experiment, the SEM experiment is used to observe the core samples with different permeabilities before and after the experiment.

Figure 3 compares the results obtained from SEM during SASP flooding. As can be seen, kaolinite in the original core is in the shape of a book page, and the white shape of a honeycomb and cotton wool in the middle part is smectite with a small amount of illite. It is apparent that kaolinite is corroded; a large number of uncorroded kaolinite fragments are present in the pores, and there is a small amount of complete kaolinite in pieces after SASP flooding.

Figure 4 compares the results obtained from SEM during SASP flooding. The results show that the surface structure is clear and the section is regular. In addition, the surface of quartz particles is more convex before SASP flooding. After corrosion, most of the smooth surface became uneven, a large number of particles accumulated on the section, the edges and corners became round, and part of the clay particles migrated. Surprisingly, most of the section was covered by a new substance (secondary quartz).

The most significant aspect of this graph is the changes in pore throat size after SASP flooding. Our study magnified the SEM to 50 μm. The results are shown in Figure 5.

A closer observation of the picture shows that there are clay particles accumulated around the pores and the pore throat in the core is narrower, which reduces the seepage capacity. This is consistent with the results of our previous seepage capacity experiments. Remarkably, we can also clearly see that the growth position of secondary quartz is on the surface of clay minerals, not quartz that exists in the original rock.

The most obvious finding to emerge from the analysis is the reservoir damage of SASP flooding. In particular, kaolinite and quartz are corroded seriously, a large amount of clay minerals are filled in the pores, and small pieces of secondary quartz are formed on the surface of the minerals. The pore throat core becomes narrower and the seepage capacity decreases.

2.4. Results of Mineral Composition. To clarify the scale formation mechanism, an X-ray diffraction (XRD) experiment was used to obtain the change of mineral composition by SASP flooding corrosion. The XRD test results are shown in Figure 6, and the mineral composition test result is shown in Table 3.

From the chart, it can be seen that the content of clay minerals becomes lower and the content of matrix mineral becomes higher due to the increase of permeability. The main results are that the content of kaolinite in clay minerals decreases, and the content of quartz in skeleton minerals increases. It is apparent that the content of matrix mineral is

https://doi.org/10.1021/acsomega.1c04925
ACS Omega 2022, 7, 1794−1802

reduced, while the content of clay mineral is increased after SASP flooding.

The findings indicate that SASP flooding has obvious damage to the reservoir. In addition, the effects on clay and matrix minerals are different. Strong evidence is found that illite/montmorillonite and chlorite contents increase obviously, while quartz and kaolinite contents decrease after SASP flooding. Previous studies have proved that NaOH more strongly attacks kaolinite than montmorillonite and illite. Our study further proves that the montmorillonite content increases obviously after SASP flooding. These results further support the idea that alkali corrodes reservoir during SASP flooding.

2.5. Corrosion Mechanism of SASP Flooding. It can thus be suggested that quartz, feldspar, and kaolinite in the reservoir can corrode with alkali during SASP flooding; there are secondary quartz and chlorite on the surface of the rock and pore throat. The corrosion mechanism is shown in Figure 7.

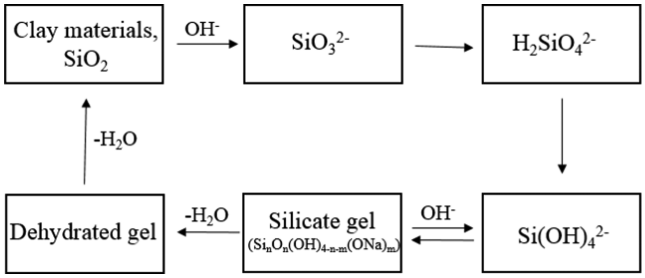

Figure 7. Corrosion mechanism process.

(1) The chemical reaction between feldspar and alkali solution is as follows

$$K(AlSi_3O_8) + Ca(Al_2Si_2O_8) + 7OH^- \rightarrow 3Al(OH)_3 \downarrow + 5SiO_3^{2-} + K^+ + Ca^{2+}$$

(2) The chemical reaction between kaolinite and alkali solution is as follows

$$Al_4(SiO_4)(OH)_8 \cdot nH_2O + 2OH^- \rightarrow 4Al(OH)_3 \downarrow + SiO_3^{2-} + H_2O$$

(3) The chemical reaction between quartz and alkali solution is as follows

$$SiO_2 + 2(OH)^- \rightarrow SiO_3^{2-} + H_2O$$

Under alkaline conditions, silicic acid is unstable and easily generates silicic acid gel. In turn, it is dehydrated to produce amorphous silica, forming a silica scale. Silicate and mineral fragments are cemented together to form new minerals such as chlorite. The reaction is as follows

$$Al_4[Si_4O_{10}](OH)_8 + 2OH^- \rightarrow Al_2[Si_4O_{10}](OH)_2 + 2Al(OH)_4^-$$

In summary, the process of scale formation is clarified by analyzing the reaction between the reservoir and the SASP system. During long-term seepage, the particles in the rock surface are disordered and corroded, corrosion deposits on pore throats, and the pore size becomes smaller. The formation process can be simply expressed as follows.

Corrosion is prone to occur with alkali for heterogeneous reservoirs with low permeability and high clay mineral content. The generated particles and detached clay particles are easy to form sediments, which block the pore throats. These results are likely to be related to a significant decrease in seepage capacity. Hence, for reservoirs with low permeability and high clay mineral content, the amount of alkali should be reduced, which can reduce the influence on reservoir damage and seepage ability during long-term SASP flooding.

3. CONCLUSIONS

The purpose of the current study was to determine the scaling mechanism in heterogeneous reservoirs with low permeability and high clay mineral content during SASP flooding. The findings from this study make several contributions to clarify the impact on the pore structure and seepage capacity of the reservoir during SASP flooding. The result can be categorized into four classes.

(1) The seepage capacity is reduced after SASP flooding. The reservoir with lower permeability will suffer more serious reservoir damage, which leads to the permeability and seepage capacity decrease.

(2) The peak of pore distribution shifts to the right, the distribution of large pores increases, and the heterogeneity of the pore structure becomes weaker after SASP flooding. Detrital particles or secondary mineral particles produced by corrosion migrate to form bridges or stay on the surface of rocks, blocking the pore throats, and therefore, the seepage ability becomes worse.

(3) SASP flooding has obvious damage to the reservoir. Strong evidence is found that illite/montmorillonite and chlorite contents increase obviously, while quartz and kaolinite contents decrease after SASP flooding.

(4) For reservoirs with low permeability and high clay mineral content, the generated corrosion particles and fallen clay particles are easy to form sediments, which may lead to a significant decrease in seepage capacity. Therefore, the amount of alkali should be reduced, which can reduce the influence on reservoir damage and seepage ability during long-term SASP flooding.

4. MATERIALS AND METHODS

4.1. Experiment Materials. *4.1.1.. Experimental Water.* The simulated formation brine was provided by Northeast Petroleum University.

4.1.2.. Experimental Chemicals. Hydrolyzed polyacrylamide (HPAM) with ~15 million molecular weight was used as a polymer; its relatively small molecular weight can prevent the high viscosity polymer from blocking pore throats. NaOH was used as the alkaline agent, and alkylbenzene sulfonate was used as a surfactant. Previous research has established that the most optimum concentrations of NaOH and alkylbenzene sulfonate are 1.2% (pH = 13.5) and 0.3%.[38] As a result, the ASP flooding slug consists of 0.3% alkylbenzene sulfonate + 1.2% NaOH + 1900 mg/L hydrolyzed polyacrylamide (HPAM).

4.1.3.. Experimental Cores. Columnar core samples with different permeabilities were selected from the oilfield, which were used for the seepage experiment. The basic parameters of core samples are shown in Table 4.

https://doi.org/10.1021/acsomega.1c04925
ACS Omega 2022, 7, 1794−1802

Table 4. Basic Parameters of Core Samples

core number	type of reservoir	permeability before flooding (mD)	porosity (%)
1	III	309	23.1
2	II	762	25.4
3	I	1635	26.7

All of the chemicals and cores were recruited by Daqing No. 3 Oilfield.

4.2. Apparatus. Traditionally, rock composition has been analyzed using an X-ray diffractometer (XRD). A scanning electron microscope (SEM) and a high-pressure mercury porosimeter were used to observe the pore structure and pore size. The core seepage experiment was carried out using a thermostat and a displacement device. Core permeability was tested by an overburden porosity meter. The experiment temperature was 45 °C.

4.3. Procedures. Before the experiment, a contract experiment should be conducted considering the polymer transport behavior. As a result, three core samples with similar permeability and porosity were selected to perform the injection experiment with polymer slug. Specific experimental steps were as follows, which were similar to the procedure of the ASP injection experiment. In addition, the polymer flooding slug consisted of 1900 mg/L hydrolyzed polyacrylamide (HPAM), which was similar to the ASP slug.

(1) The first step in this process was to dry the core samples and measure the permeability of the core samples.
(2) Prior to vacuuming the samples until the degree reached 98%, they were saturated with formation water, and then the pore volume was calculated.
(3) Then, 3 PV water flooding was injected until the water cut reached 98%, followed by the injection of polymer slug. The total injection volume was 30 PV and the injection rate was 0.1 mL/min. The fluid production and pressure changes should be recorded.
(4) Once production increased steadily, subsequent water flooding (3 PV) was injected to displace most of the polymer in the core until the pressure was unchanged. Then, the fluid production and pressure changes were recorded.

To determine the permeability changes after SASP flooding, a total of three cores with different permeabilities were selected. In an attempt to avoid the interference of polymer and asphaltene adsorption in crude oil, which may affect the results of seepage experiments, the cores are not saturated with crude oil before SASP flooding. The water flooding process was repeated after SASP flooding to displace the polymer and the surfactant remaining in the pores and throats. All of the procedures should ensure that the samples are clean. Specific experimental steps are as follows

(1) The first step in this process was to dry the core samples and cut them into two slices with a thickness of 2−4 mm. Then, the permeability of the core samples was measured.
(2) Prior to vacuuming the samples until the degree reaches 98%, they were saturated with formation water, and then the pore volume was calculated.
(3) Afterward, 3 PV water flooding was injected until the water cut reached 98%, followed by the injection of alkaline−surfactant−polymer slug. The total injection volume was 30 PV and the injection rate was 0.1 mL/min. The fluid production and pressure changes should be recorded.
(4) Once production increased steadily, subsequent water flooding (3 PV) was injected to displace most of the polymer and surfactant in the core until the pressure was unchanged.
(5) Following this treatment, the core samples were dried and the core was cut into two slices with a thickness of 2−4 mm.
(6) When the flooding experiment was finished, permeability was calculated at each stage.
(7) The final stage of the study was to compare the structure and mineral composition with the SEM, X-ray diffractometer, and high-pressure mercury porosimeter. Then, the experimental results were compared and evaluated. The experimental process diagram is shown in Figure 8.

AUTHOR INFORMATION

Corresponding Author

Huiying Zhong − *Key Laboratory for Enhanced Oil & Gas Recovery of the Ministry of Education, Northeast Petroleum University, Daqing 163318 Heilongjiang, P. R. China*; Email: zhhy987@126.com

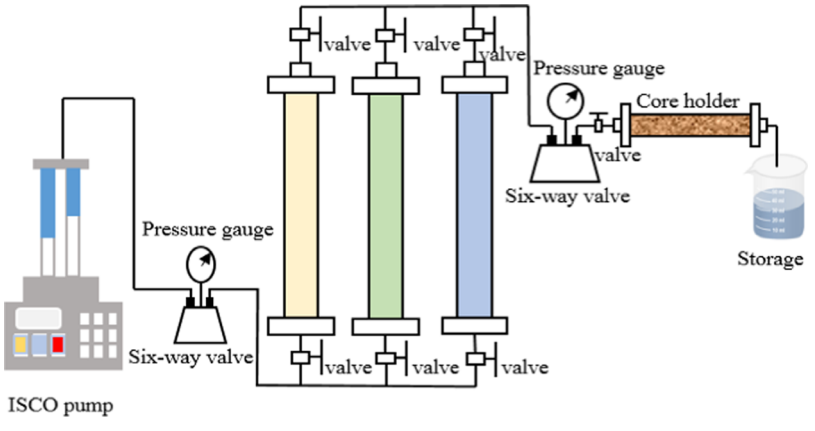

Figure 8. Experiment process diagram.

https://doi.org/10.1021/acsomega.1c04925
ACS Omega 2022, 7, 1794−1802

Authors

Runnan Zhou − *Key Laboratory for Enhanced Oil & Gas Recovery of the Ministry of Education, Northeast Petroleum University, Daqing 163318 Heilongjiang, P. R. China;* orcid.org/0000-0001-9629-1903

Peng Ye − *ASP Flooding Project Department, Daqing Oilfield Company Limited, Daqing 163318 Heilongjiang, P. R. China*

Jianguang Wei − *Key Laboratory of Continental Shale Hydrocarbon Accumulation and Efficient Development, Ministry of Education, Institute of Unconventional Oil & Gas, Northeast Petroleum University, Daqing 163318 Heilongjiang, P. R. China*

Dong Zhang − *Key Laboratory for Enhanced Oil & Gas Recovery of the Ministry of Education, Northeast Petroleum University, Daqing 163318 Heilongjiang, P. R. China; Postdoctoral Research Station, Daqing Petroleum Administration Bureau, Daqing 163318 Heilongjiang, P. R. China*

Lianbin Zhong − *ASP Flooding Project Department, Daqing Oilfield Company Limited, Daqing 163318 Heilongjiang, P. R. China*

Tianyu Jiao − *ASP Flooding Project Department, Daqing Oilfield Company Limited, Daqing 163318 Heilongjiang, P. R. China*

Complete contact information is available at: https://pubs.acs.org/10.1021/acsomega.1c04925

Notes

The authors declare no competing financial interest.

■ ACKNOWLEDGMENTS

This research was funded by the Postdoctoral Research Foundation of China (2021M690529).

■ ABBREVIATIONS

ASP, alkaline−surfactant−polymer; EOR, enhance oil recovery; SASP, strong alkali−surfactant−polymer; OOIP, original oil in place; SEM, scanning electron microscope

■ REFERENCES

(1) Kamari, A.; Nikookar, M.; Sahranavard, L.; Mohammadi, A. H. Efficient Screening of Enhanced Oil Recovery Methods and Predictive Economic Analysis. *Neural Comput. Appl.* **2014**, *25*, 815−824.

(2) Shaker Shiran, B.; Skauge, A. Enhanced oil recovery (EOR) by combined low salinity water/polymer flooding. *Energy Fuels* **2013**, *27*, 1223−1235.

(3) Shi, F.; Wu, J.; Jin, Z.; Zhuang, T.; Yin, S.; Zhao, B. Preparation and application of targeted response nanocapsules for oil displacement. *Energy Rep.* **2021**, *7*, 6222−6233.

(4) Zhang, Y.; Lu, F.; Cai, M.; Yang, Y.; Li, Ji.; Guo, Z.; et al. Physical simulation experiments of remaining oil distribution and production in alluvial fans controlled by dynamic and static factors. *J. Pet. Sci. Eng.* **2020**, *195*, No. 107714.

(5) Zhou, R.; Zhang, D.; Wei, J. Experiment on the profile control effect of different strength gel systems in heterogeneous reservoir. *Energy Rep.* **2021**, *7*, 6023−6030.

(6) Li, J.; Niu, L.; Lu, X. Performance of ASP compound systems and effects on flooding efficiency. *J. Pet. Sci. Eng.* **2019**, *178*, 1178−1193.

(7) Yang, E.; Fang, Y.; Liu, Y.; Li, Z.; Wu, J. Research and application of microfoam selective water plugging agent in shallow low -temperature reservoirs. *J. Pet. Sci. Eng.* **2020**, *193*, 107354.

(8) Muggeridge, A.; Cockin, A.; Webb, K.; Frampton, H.; Collins, I.; Moulds, T.; Salino, P. Recovery rates, enhanced oil recovery and technological limits. *Philos. Trans. R. Soc. A: Math. Phys. Eng. Sci.* **2014**, *372*, No. 20120320.

(9) Li, S.; Ge, Y.; Zang, R. A Novel Interacting Multiple-Model Method and Its Application to Moisture Content Prediction of ASP Flooding. *Comput. Model. Eng. Sci.* **2018**, *114*, 95−116.

(10) Wu, Y.; Mahmoudkhani, A.; Watson, P. In *Development of New Polymers With Better Performance Under Conditions of High Temperature and High Salinity*. SPE EOR Conference at Oil and Gas West Asia, Muscat, Oman, 2012; pp 16−18.

(11) Guo, H.; Li, Y.; Kong, D.; Ma, R.; Li, B.; Wang, F. Lesson learned from alkali/surfactant/polymer-flooding field tests in China. *SPE Reservoir Eval. Eng.* **2019**, *22*, 78−99.

(12) Kudaibergenov, S.; Shakhvorostov, A.; Gussenov, I.; Seilkhanov, T.; Nuraje, N. Application of novel hydrophobically modified polybetaines based on alkylaminocrotonates and methacrylic acid as pour point depressants and ASP flooding agent. *Polym. Bull.* **2019**, *76*, 5129−5147.

(13) Cong, Z.; Li, Y.; Pan, Y.; Liu, B.; Shi, Y.; Wei, J.; Li, W. Study on CO_2 Foam Fracturing Model and Fracture Propagation Simulation. *Energy* **2022**, *238*, No. 121778.

(14) Wang, D.; Cheng, J. The application of polymer oil removal technology in Daqing oilfield. *J. Pet.* **2006**, *26*, 74−78.

(15) Lee, Y.; Lee, W.; Jang, Y.; Sung, W. Oil recovery by low-salinity polymer flooding in carbonate oil reservoirs. *J. Pet. Sci. Eng.* **2019**, *181*, No. 106211.

(16) Zhang, C.; Wang, P.; Song, G. Study on enhanced oil recovery by Multi-component foam flooding. *J. Pet. Sci. Eng.* **2019**, *177*, 181−187.

(17) Zhong, H.; Yang, T.; Yin, H.; Lu, J.; Zhang, K.; Fu, C. Role of Alkali Type in Chemical Loss and ASP-Flooding Enhanced Oil Recovery in Sandstone Formations. *SPE Reservoir Eval. Eng.* **2020**, *23*, 431−445.

(18) Azad, M. S. IFT Role on Oil Recovery During Surfactant Based EOR Methods. In *Surfactants in Upstream E&P*; Springer: Cham, 2021; pp 115−148.

(19) Taber, J. J.; Martin, F. D.; Seright, R. S. EOR screening criteria revisited. 1. Introduction to screening criteria and enhanced recovery field projects. *SPE Reservoir Eng.* **1997**, *8*, 189−198.

(20) Sun, C.; Guo, H.; Li, Y.; Jiang, G.; Ma, R. Alkali Effect on Alkali-Surfactant-Polymer (ASP) Flooding Enhanced Oil Recovery Performance: Two Large-Scale Field Tests' Evidence. *J. Chem.* **2020**, *2020*, No. 2829565.

(21) Wang, D.; Yin, D.; Gong, X. Numerical simulation of microemulsion flooding in low permeability reservoir. *J. Chem.* **2019**, *2019*, No. 5021473.

(22) Sui, X.; Chen, Z.; Ivan, K.; Han, X.; Yu, J.; Zhang, G. Alkaline-surfactant-polymer flooding of active oil under reservoir conditions. *Fuel* **2020**, *262*, No. 116647.

(23) Sun, L.; Wu, X.; Zhou, W.; Li, X.; Han, P. Technologies of enhancing oil recovery by chemical flooding in Daqing oilfield, NE China. *Pet. Explor. Dev.* **2018**, *45*, 673−684.

(24) Gong, H.; Zhang, H.; Xu, L.; et al. Further enhanced oil recovery by branched-preformed particle gel/HPAM/surfactant mixed solutions after polymer flooding in parallel-sandpack models. *RSC Adv.* **2017**, *7*, 39564−39575.

(25) Liu, M. Study on recovery feature of the weak base ASP flooding. *IOP Conf. Ser.: Earth Environ. Sci.* **2019**, *300*, No. 022060.

(26) Tackie-Otoo, B. N.; Mohammed, M. A. A.; Nurudeen, Y.; Negash, B. M. Alternative chemical agents for alkalis, surfactants and polymers for enhanced oil recovery: Research trend and prospects. *J. Pet. Sci. Eng.* **2020**, *187*, No. 106828.

(27) Gao, Q.; Zhong, C.; Han, P.; Cao, R.; Jiang, G. Synergistic Effect of Alkali-Surfactant-Polymer and Preformed Particle Gel on Profile Control after Polymer Flooding in Heterogeneous Reservoirs. *Energy Fuels* **2020**, *34*, 15957−15968.

(28) Nandi, R.; Laskar, S.; Saha, B. Surfactant-promoted enhancement in bioremediation of hexavalent chromium to trivalent chromium by naturally occurring wall algae. *Res. Chem. Intermed.* **2017**, *43*, 1619−1634.

(29) Li, Y.; Kong, B.; Li, C. Dynamic characteristics of synergistic effect between profile control technology throughout flooding and ASP flooding. *Acta Ecol. Sin.* **2018**, *39*, 697−702.
(30) Li, Y.; Long, M.; Tang, J.; Chen, M.; Fu, X. A Hydraulic Fracture Height Mathematical Model Considering the Influence of Plastic Region at Fracture Tip. *Pet. Explor. Dev.* **2020**, *47*, 184−195.
(31) Xie, K.; Cao, B.; Lu, X.; et al. Matching between the diameter of the aggregates of hydrophobically associating polymers and reservoir pore-throat size during polymer flooding in an offshore oilfield. *J. Pet. Sci. Eng.* **2019**, *177*, 558−569.
(32) Panthi, K.; Sharma, H.; Mohanty, K. ASP flood of a viscous oil in a carbonate rock. *Fuel* **2016**, *164*, 18−27.
(33) Li, Y.; Jia, D.; Rui, Z.; Peng, J.; Fu, C.; Zhang, J. Evaluation Method of Rock Brittleness Based on Statistical Constitutive Relations for Rock Damage. *J. Pet. Sci. Eng.* **2017**, *153*, 123−132.
(34) Zhang, J.; Li, Y.; Pan, Y.; Wang, X.; Yan, M.; Shi, X.; Zhou, X.; Li, H. Experiments and Analysis on the Influence of Multiple Closed Cemented Natural Fractures on Hydraulic Fracture Propagation in a Tight Sandstone Reservoir. *Eng. Geol.* **2021**, *281*, No. 105981.
(35) Li, J.; Jiang, H.; Wang, C.; Zhao, Y.; Gao, Y.; Pei, Y.; et al. Pore-scale investigation of microscopic remaining oil variation characteristics in water-wet sandstone using CT scanning. *J. Nat. Gas Sci. Eng.* **2017**, *48*, 36−45.
(36) Seright, R. S. How Much Polymer Should Be Injected During a Polymer Flood? Review of Previous and Current Practices. *SPE J.* **2017**, *22*, 1−18.
(37) Wang, D.; Li, C.; Seright, R. Laboratory Evaluation of Polymer Retention in a Heavy Oil Sand for a Polymer Flooding Application on Alaska's North Slope. *SPE J.* **2020**, *25*, 1842−1856.
(38) Zhu, Y. In *Current Developments and Remaining Challenges of Chemical Flooding EOR Techniques in China*. Proceedings of the SPE Asia Pacific Enhanced Oil Recovery Conference, 2015.

https://doi.org/10.1021/acsomega.1c04925
ACS Omega 2022, 7, 1794−1802